Published in final edited form as:
Heart Rhythm. 2010 ; 7(2): 199–205. doi:10.1016/j.hrthm.2009.10.012.

KCNE2 modulation of Kv4.3 current and its potential role in fatal rhythm disorders

Jie Wu, PhD[*], **Wataru Shimizu, MD, PhD**[†], **Wei-Guang Ding, MD, PhD**[‡], **Seiko Ohno, MD, PhD**[§], **Futoshi Toyoda, PhD**[‡], **Hideki Itoh, MD, PhD**[¶], **Wei-Jin Zang, MD, PhD**[*], **Yoshihiro Miyamoto, MD, PhD**[‖], **Shiro Kamakura, MD, PhD**[†], **Hiroshi Matsuura, MD, PhD**[‡], **Koonlawee Nademanee, MD, FACC**[#], **Josep Brugada, MD**[**], **Pedro Brugada, MD**[††], **Ramon Brugada, MD, PhD, FACC**[‡‡], **Matteo Vatta, PhD**[§§,¶¶], **Jeffrey A. Towbin, MD, FAAP, FACC**[§§], **Charles Antzelevitch, PhD, FACC, FAHA, FHRS**[‖‖], and **Minoru Horie, MD, PhD**[¶]

[*]Pharmacology Department, Medical School of Xi'an Jiaotong University. Xi'an, Shaanxi, China

[†]Division of Cardiology, Department of Internal Medicine, National Cardiovascular Center, Suita, Japan

[‡]Department of Physiology, Shiga University of Medical Science, Ohtsu, Japan

[§]Department of Cardiovascular Medicine, Kyoto University of Graduate School of Medicine, Kyoto, Japan

[¶]Department of Cardiovascular Medicine, Shiga University of Medical Science, Shiga, Japan

[‖]Laboratory of Molecular Genetics, National Cardiovascular Center, Suita, Japan

[#]Department of Medicine (Cardiology), University of Southern California, Los Angeles, California

[**]Cardiovascular Institute, Hospital Clinic, University of Barcelona, Barcelona, Spain

[††]Heart Rhythm Management Centre, Free University of Brussels (UZ Brussel) VUB, Brussels, Belgium

[‡‡]School of Medicine, Cardiovascular Genetics Center, University of Girona, Girona, Spain

[§§]Departments of Pediatrics, Baylor College of Medicine, Houston, Texas

[¶¶]Department of Molecular Physiology and Biophysics, Baylor College of Medicine, Houston, Texas

[‖‖]Masonic Medical Research Laboratory, Utica, New York

Abstract

Background—The transient outward current I_{to} is of critical importance in regulating myocardial electrical properties during the very early phase of the action potential. The auxiliary β subunit *KCNE2* recently was shown to modulate I_{to}.

Objective—The purpose of this study was to examine the contributions of *KCNE2* and its two published variants (M54T, I57T) to I_{to}.

Methods—The functional interaction between Kv4.3 (α subunit of human I_{to}) and wild-type (WT), M54T, and I57T *KCNE2*, expressed in a heterologous cell line, was studied using patch-clamp techniques.

Address reprint requests and correspondence: Dr. Minoru Horie, Department of Cardiovascular and Respiratory Medicine, Shiga University of Medical Science, Otsu, Shiga 520-2192, Japan. horie@belle.shiga-med.ac.jp.
The first two authors contributed equally to the original concept and the authorship of this study.

Results—Compared to expression of Kv4.3 alone, co-expression of WT *KCNE2* significantly reduced peak current density, slowed the rate of inactivation, and caused a positive shift of voltage dependence of steady-state inactivation curve. These modifications rendered Kv4.3 channels more similar to native cardiac I_{to}. Both M54T and I57T variants significantly increased I_{to} current density and slowed the inactivation rate compared with WT *KCNE2*. Moreover, both variants accelerated the recovery from inactivation.

Conclusion—The study results suggest that *KCNE2* plays a critical role in the normal function of the native I_{to} channel complex in human heart and that M54T and I57T variants lead to a gain of function of I_{to}, which may contribute to generating potential arrhythmogeneity and pathogenesis for inherited fatal rhythm disorders.

Keywords

Cardiac arrhythmia; M54T variation; I57T variation; *KCNE2*; Kv4.3; Sudden cardiac death

Introduction

Classic voltage-gated K^+ channels consist of four pore-forming (α) subunits that contain the voltage sensor and ion selectivity filter1,2 and accessory regulating (β) subunits.3 *KCNE* family genes encode several kinds of β subunits consisting of single transmembrane-domain peptides that co-assemble with α subunits to modulate ion selectivity, gating kinetics, second messenger regulation, and the pharmacology of K^+ channels. Association of the *KCNE1* product minK with the α subunit Kv7.1 encoding *KCNQ1* forms the slowly activating delayed rectifier K^+ current I_{Ks} in the heart.4,5 In contrast, association of the *KCNE2* product MiRP1 with the human ether-a-go-go related gene (HERG) forms the cardiac rapid delayed rectifier K^+ current I_{Kr}.6

Abbott et al reported that three *KCNE2* variants (Q9E, M54T, I57T) caused a loss of function in I_{Kr} and thereby were associated with the congenital or drug-induced long QT syndrome.6,7 However, the reported QTc values in two index patients with M54T and I57T variants, both located in the transmembrane segment of MiRP1, were only mildly prolonged (390–500 ms and 470 ms).6 We recently identified the same missense *KCNE2* variant, I57T, in which isoleucine was replaced by threonine at codon 57, in three unrelated probands showing a Brugada type 1 ECG. These findings are difficult to explain on the basis of a loss of function in I_{Kr}, thus leading us to explore other mechanisms.

Recent studies have demonstrated that interaction between α and β subunits (*KCNEs*) of voltage-gated K^+ channel is more promiscuous; for example, MiRP1 has been shown to interact with Kv7.1,8–10 HCN1,11 Kv2.1,12 and Kv4.2.13 These studies suggest that MiRP1 may also co-associate with Kv4.3 and contribute to the function of transient outward current (I_{to}) channels.14 Indeed, a recent study reported that I_{to} is diminished in *kcne2* (−/−) mice.15

In the human heart, I_{to} currents are of critical importance in regulating myocardial electrical properties during the very early phase of the action potential and are thought to be central to the pathogenesis of Brugada-type ECG manifestations.16 Antzelevitch et al demonstrated that a gain of function in I_{to} secondary to a mutation in *KCNE3* contributes to a Brugada phenotype by interacting with Kv4.3 and thereby promoting arrhythmogenicity.14

We hypothesized that mutations in *KCNE2* may have similar actions and characterize the functional consequences of interaction of wild-type (WT) and two mutant (I57T, M54T) MiRP1 with Kv4.317,18 using heterologous co-expression of these α and β subunits in Chinese hamster ovary (CHO) cells.

Methods

Heterologous expression of hKv4.3 and β subunits in CHO cells

Full-length cDNA fragment of *KCNE2* in pCR3.1 vector10 was subcloned into pIRES-CD8 vector. This expression vector is useful in cell selection for later electrophysiologic study (see below). Two *KCNE2* mutants (M54T, I57T) were constructed using a Quick Change II XL site-directed mutagenesis kit according to the manufacturer's instructions (Stratagene, La Jolla, CA, USA) and subcloned to the same vector. Two *KCNE2* mutants were fully sequenced (ABI3100×, Applied Biosystems, Foster City, CA, USA) to ensure fidelity. Full-length cDNA encoding the short iso-form of human Kv4.3 subcloned into the pIRES-GFP (Clontech, Palo Alto, CA, USA) expression vector was kindly provided by Dr. G.F. Tomaselli (Johns Hopkins University). Full-length cDNA encoding Kv channel-interacting protein (*KCNIP2*) subcloned into the PCMV-IRS expression vector was a kind gift from Dr. G.-N. Tseng (Virginia Commonwealth University). *KCND3* was transiently transfected into CHO cells together with *KCNE2* (or M54T or I57T) cDNA at equimolar ratio (*KCND3* 1.5 μg, *KCNE2* 1.5 μg) using Lipofectamine (Invitrogen Life Technologies, Carlsbad, CA, USA) according to the manufacturer's instructions. In one set of experiments, we also co-transfected equimolar levels of KChIP2b (*KCND3* 1.5 μg, *KCNE2* 1.5 μg, *KCNIP2* 1.5 μg). The transfected cells were then cultured in Ham's F-12 medium (Nakalai Tesque, Inc., Kyoto, Japan) supplemented with 10% fetal bovine serum (JRH Biosciences, Inc., Lenexa, KS, USA) and antibiotics (100 international units per milliliter penicillin and 100 μg/mL streptomycin) in a humidified incubator gassed with 5% CO_2 and 95% air at 37°C. The cultures were passaged every 4 to 5 days using a brief trypsin-EDTA treatment. The trypsin-EDTA treated cells were seeded onto glass coverslips in a Petri dish for later patch-clamp experiments.

Electrophysiologic recordings and data analysis

After 48 hours of transfection, a coverslip with cells was transferred to a 0.5-mL bath chamber at 25°C on an inverted microscope stage and perfused at 1 to 2 mL/min with extracellular solution containing the following (in mM): 140 NaCl, 5.4 KCl, 1.8 $CaCl_2$, 0.5 $MgCl_2$, 0.33 NaH_2PO_4, 5.5 glucose, and 5.0 HEPES; pH 7.4 with NaOH. Cells that emitted green fluorescence were chosen for patch-clamp experiments. If co-expressed with *KCNE2* (or its mutants), the cells were incubated with polystyrene microbeads pre-coated with anti-CD8 antibody (Dynabeads M450, Dynal, Norway) for 15 minutes. In these cases, cells that emitted green fluorescence and had attached beads were chosen for electrophysiologic recording. Whole-cell membrane currents were recorded with an EPC-8 patch-clamp amplifier (HEKA, Lambrecht, Germany), and data were low-pass filtered at 1 kHz, acquired at 5 kHz through an LIH-1600 analog-to-digital converter (HEKA), and stored on hard disk using PulseFit software (HEKA). Patch pipettes were fabricated from borosilicate glass capillaries (Narishige, Tokyo, Japan) using a horizontal microelectrode puller (P-97, Sutter Instruments, Novato, CA, USA) and the pipette tips fire-polished using a microforge. Patch pipettes had a resistance of 2.5 to 5.0 MΩ when filled with the following pipette solution (in mM): 70 potassium aspartate, 50 KCl, 10 KH_2PO_4, 1 $MgSO_4$, 3 Na_2-ATP (Sigma, Japan, Tokyo), 0.1 Li_2-GTP (Roche Diagnostics GmbH, Mannheim, Germany), 5 EGTA, and 5 HEPES (pH 7.2).

Cell membrane capacitance (C_m) was calculated from 5 mV-hyperpolarizing and depolarizing steps (20 ms) applied from a holding potential of −80 mV according to Equation 1 19:

$$C_m=\tau_c I_0/\Delta V_m(1-I_\infty/I_0), \quad (1)$$

where τ_c = time constant of capacitance current relaxation, I_0 = initial peak current amplitude, ΔV_m = amplitude of voltage step, and I_∞ = steady-state current value. Whole-cell currents were elicited by a family of depolarizing voltage steps from a holding potential of −80 mV. The difference between the peak current amplitude and the current at the end of a test pulse (1-second duration) was referred to as the transient outward current. To control for cell size variability, currents were expressed as densities (pA/pF).

Steady-state activation curves were obtained by plotting the normalized conductance as a function of peak outward potentials. Steady-state inactivation curves were generated by a standard two-pulse protocol with a conditioning pulse of 500-ms duration and obtained by plotting the normalized current as a function of the test potential. Steady-state inactivation/activation kinetics were fitted to the following Boltzmann equation (Eq. 2):

$$Y(V)=1/(1+\exp[(V_{1/2}-V)/k]), \quad (2)$$

where Y = normalized conductance or current, $V_{1/2}$ = potential for half-maximal inactivation or activation, respectively, and k = slope factor.

Data relative to inactivation time constants, time to peak, and mean current levels were obtained by using current data recorded at +50 mV or +20 mV. Recovery from inactivation was assessed by a standard paired-pulse protocol: a 400-ms test pulse to +50 mV (P1) followed by a variable recovery interval at −80 mV and then a second test pulse to +50 mV (P2). Both the inactivation time constants and the time constant for recovery from inactivation were determined by fitting the data to a single exponential (Eq. 3):

$$I(t)\ (\text{or}P2/P1)=A+B_{\exp}(-t/\tau), \quad (3)$$

where I(t) = current amplitude at time t, A and B = constants, and τ = inactivation time constant or time constant for recovery from inactivation. For measurement of recovery from inactivation, the plot of P2/P1 instead of I(t) was used.

All data were given as mean ± SEM. Statistical comparisons between two groups were analyzed using Student's unpaired t-test. Comparisons among multiple groups were analyzed using analysis of variance followed by Dunnett test. $P < .05$ was considered significant.

Results

Effects of *KCNE2* on Kv4.3 currents and its gating kinetics

WT *KCNE2* initially was co-expressed with *KCND3*, the gene encoding Kv4.3, the *α* subunit of the I_{to} channel,[17,18] in CHO cells. Figure 1A shows representative whole-cell current traces recorded from cells transfected with *KCND3* and co-transfected with (right) or without (left) *KCNE2*. Cells expressing Kv4.3 channels alone showed rapidly activating and inactivating currents. Co-expression of *KCNE2* significantly reduced peak current densities as summarized in the current–voltage relationship curve shown in Figure 1B and slowed both activation and inactivation kinetics (Table 1). Figure 1C (left) shows mean time intervals from the onset of the pulse to maximum current (time to peak), whereas the right panel shows time constants of inactivation (at +20 mV) obtained using Equation 3. Thus, co-transfection of *KCNE2* significantly increased both the time to peak and the time constant.

In contrast, *KCNE2* did not affect the voltage dependence of steady-state activation as assessed by plotting the normalized conductance as a function of test potential (Figure 1D). Fitting to the Boltzmann equation (Eq. 2) yielded half-maximal activation potentials of −6.5

± 2.1 mV for Kv4.3 alone (open circles) and −5.5 ± 1.7 mV for Kv4.3 + *KCNE2* channels (filled circles, *P* = NS; Table 1). These findings are consistent with those previously reported for studies using *Xenopus* oocytes, CHO cells, and HEK293 cells.20,21

KCNE2 co-expression also caused a positive shift (approximately + 5 mV) of voltage dependence of steady-state inactivation. Steady-state inactivation was assessed using a double-step pulse method (Figure 2A, inset). Peak outward currents recorded at various levels of prepulse (Figure 2A) were normalized by that measured after a 500-ms prepulse at −90 mV and are plotted as a function of prepulse test potentials (Figure 2B). Half-inactivation potentials of steady-state inactivation, determined by fitting data to the Boltzmann equation (Eq. 2), were −46.0 ± 1.3 mV for Kv4.3 (open circles) and −40.8 ± 1.7 mV for Kv4.3 + *KCNE2* (filled circles, *P* <.01), consistent with the observation of Tseng's group.13

A double-pulse protocol (Figure 3A, inset) was used to test the effect of *KCNE2* co-expression on the time course for recovery from inactivation. Figure 3A shows the time course of recovery of Kv4.3 alone (open circles) and Kv4.3 + *KCNE2* (filled circles). Mean time constants for recovery from inactivation were not significantly different, indicating that co-transfection of *KCNE2* did not affect the time course of recovery from inactivation.

Effects of *KCNE2* on Kv4.3 + KChIP2b current and its gating kinetics

For human native cardiac I_{to}, KChIP2 has been shown to serve as a principal β subunit.22–25 Accordingly, in another series of experiments, we examined the effect of WT and mutant *KCNE2* on Kv4.3 + KChIP2b current. Consistent with previous reports, in the presence of KChIP2, Kv4.3 currents showed a significantly faster recovery from inactivation (Figure 3B and Table 1).26,27 Co-expression of WT *KCNE2* produced similar changes on Kv4.3 + KChIP2b current as on Kv4.3 current (Table 1). Kv4.3 + KChIP2b current recovery from inactivation was further accelerated: average time constant was 89.2 ± 6.5 ms for Kv4.3 + KChIP2b alone (open circles) and 60.2 ± 8.4 ms for Kv4.3 + KChIP2b + *KCNE2* (filled circles, *P* <.05). In 16 of 21 cells transfected with *KCNE2*, we observed an “overshoot” phenomenon, which is commonly seen during recording of native I_{to} in human ventricular myocytes.28

KCNE2 variants increase Kv4.3 + KChIP2b current and alter its gating kinetics

The I57T variant was first identified in an asymptomatic middle-aged woman with very mild QT prolongation.6 In addition to this variant, the authors reported another *KCNE2* variant of the transmembrane segment (M54T) that was associated with ventricular fibrillation during exercise in a middle-aged woman. This patient appeared to show a wide range of QTc interval (390–500 ms). Therefore, we tested the functional effects of these two transmembrane *KCNE2* variants on Kv4.3 + KChIP2b currents.

The three panels of Figure 4A show three sets of current traces elicited by depolarizing pulses from a holding potential of −80 mV in cells co-transfected with WT (a), I57T (b), or M54T (c) *KCNE2*. Neither variant caused a significant shift of half-maximal activation voltage: −7.4 ± 1.4 mV (n = 8) for co-expression of WT *KCNE2*, −6.1 ± 1.5 mV (n = 8) for I57T, and −6.6 ± 1.6 mV (n = 8) for M54T. Both variants significantly increased I_{to} density: 125.0 ± 10.6 pA/pF in WT *KCNE2* (n = 21), 178.1 ± 12.1 pA/pF with I57T (n = 9), and 184.3 ± 27.9 pA/pF with M54T (n = 9, Figure 4C).

Figure 5A shows the three traces depicted in Figure 4B normalized to their peak current level. This representation shows that the time course of inactivation of the two variant currents is slowed. The current decay was fitted by Equation 3 and the time constants (at + 20 mV) summarized in Figure 5A, panel b. Finally, Figure 5B shows that the time constants

of recovery of the two mutant channels from inactivation were significantly reduced. Thus, compared to WT *KCNE2*, recovery of reconstituted Kv4.3 + KChIP2b channels from inactivation was significantly accelerated with both I57T and M54T mutants.

Discussion

Kv4.3/KChIP2/MiRP1 complex can recapitulate the native I_{to}

In the present study, co-expression of WT *KCNE2* produced changes in kinetic properties (Figures 1–3 and Table 1) that led to close recapitulation of native cardiac I_{to}.28,29 Notably, in addition to causing a positive shift of steady-state inactivation (Figure 2), *KCNE2* co-expression hastened the recovery of Kv4.3 + KChIP2b channels from inactivation (Figure 3). These modifications rendered Kv4.3 + KChIP2b channels more similar to native cardiac I_{to}, suggesting that *KCNE2* may be an important component of the native I_{to} channel complex. In contrast to a previous observation in HEK293 cells,21 *KCNE2* co-expression decreased the current density of Kv4.3 and Kv4.3 + KChIP2b channel current in the present study, which seems to be a more reasonable result as the native I_{to} density reportedly was smaller in isolated human heart.28 *KCNE2* co-expression has also been shown to reduce the density of Kv7.1[8,9] and HERG[6,7] channels.

Similar to the result of Deschenes and Tomaselli,21 we failed to observe an overshoot during recovery from inactivation when *KCNE2* was co-expressed with Kv4.3 (Figure 3A), which is in contrast to the report of another group.13 However, co-expression of *KCNE2* with Kv4.3 + KChIP2 channels produced an overshoot (Figure 3B), consistent with the report of Wettwer's group.25 Wettwer et al also found that other *KCNE* subunits either were ineffective or induced only a small overshoot in CHO cells. Therefore, both MiRP1 and KChIP2 subunits are sufficient and necessary to recapitulate native I_{to} in the heart. Considering that the overshoot phenomenon has been described only in human ventricular I_{to} channels of the epicardial but not endocardial region,28 these results may further implicate participation of MiRP1 and KChIP2 in the I_{to} channel complex in epicardium.

KCNE2 variants may alter the arrhythmogenic substrate by modulating I_{to}

Heterologous expression in CHO cells was conducted to examine the functional effects of I57T and M54T variants on Kv4.3 + KChIP2 channels. Both I57T and M54T *KCNE2* variants significantly (1) increased peak transient outward current density (Figure 4), (2) slowed the decay of the reconstituted I_{to} (Figure 5A), and (3) accelerated its recovery from inactivation (Figure 5B). Both variants thus caused an important gain of function in human I_{to}. These sequence changes may play a role in modulating I_{to} and thereby predispose to some inherited fatal rhythm disorders.

Functional effects on I_{to} induced by I57T and M54T resemble each other, increasing I_{to} density and accelerating its recovery from inactivation. The gain of function in I_{to} opposes the fast inward Na^+ currents during phase 0 of the action potential, leading to all or none repolarization at the end of phase 1 and loss of the epicardial action potential dome, thus promoting phase 2 reentry and fatal ventricular arrhythmias.30

Another *KCNE2* variant (M54T) associated with fatal arrhythmias was first identified in a woman who had a history of ventricular fibrillation and varied QT intervals.6 It is possible that her arrhythmia was also related to a gain of function in I_{to} secondary to this variation in *KCNE2*. Interestingly, the I57T variant has been reported to produce a loss of function of HERG or Kv7.1 channels, thereby predisposing to long QT syndrome,6,8 indicating that the same *KCNE2* variant could cause two different cardiac rhythm disorders, similar to long QT syndrome and Brugada syndrome caused by *SCN5A* mutations.31,32

Acknowledgments

This study was supported by grants from the Ministry of Education, Culture, Sports, Science, Technology Leading Project for Biosimulation to Dr. Horie; Health Sciences Research grants (H18-Research on Human Genome-002) from the Ministry of Health, Labour and Welfare, Japan to Drs. Shimizu and Horie; the National Natural Science Foundation of China (Key Program, No.30930105; General Program, No. 30873058, 30770785) and the National Basic Research Program of China (973 Program, No. 2007CB512005) and CMB Distinguished Professorships Award (No. F510000/G16916404) to Dr. Zang; and National Institutes of Health Grant HL47678 and Free and Accepted Masons of New York State and Florida to Dr. Antzelevitch.

References

1. Kass RS, Freeman LC. Potassium channels in the heart: cellular, molecular, and clinical implications. Trends Cardiovasc Med. 1993; 3:149–159. [PubMed: 21244942]
2. MacKinnon R. Determination of the subunit stoichiometry of a voltage-activated potassium channel. Nature. 1991; 350:232–235. [PubMed: 1706481]
3. Abbott GW, Goldstein SA. A superfamily of small potassium channel subunits: form and function of the MinK-related peptides (MiRPs). Q Rev Biophys. 1998; 31:357–398. [PubMed: 10709243]
4. Barhanin J, Lesage F, Guillemare E, Fink M, Lazdunski M, Romey G. KvLQT1 and IsK (minK) proteins associate to form the I_{Ks} cardiac potassium current. Nature. 1996; 384:78–80. [PubMed: 8900282]
5. Sanguinetti MC, Curran ME, Zou AR, et al. Coassembly of KvLQT1 and minK (I_{Ks}) proteins to form cardiac I_{Ks} potassium channel. Nature. 1996; 384:80–83. [PubMed: 8900283]
6. Abbott GW, Sesti F, Splawski I, et al. MiRP1 forms I_{Kr} potassium channels with HERG and is associated with cardiac arrhythmia. Cell. 1999; 97:175–187. [PubMed: 10219239]
7. Sesti F, Abbott GW, Wei J, et al. A common polymorphism associated with antibiotic-induced cardiac arrhythmia. Proc Natl Acad Sci U S A. 2000; 97:10613–10618. [PubMed: 10984545]
8. Tinel N, Diochot S, Borsotto M, Lazdunski M, Barhanin J. *KCNE2* confers background current characteristics to the cardiac KCNQ1 potassium channel. EMBO J. 2000; 19:6326–6330. [PubMed: 11101505]
9. Wu DM, Jiang M, Zhang M, Liu XS, Korolkova YV, Tseng GN. *KCNE2* is colocalized with KCNQ1 and *KCNE1* in cardiac myocytes and may function as a negative modulator of $I_{(Ks)}$ current amplitude in the heart. Heart Rhythm. 2006; 3:1469–1480. [PubMed: 17161791]
10. Toyoda F, Ueyama H, Ding WG, Matsuura H. Modulation of functional properties of KCNQ1 channel by association of KCNE1 and KCNE2. Biochem Biophys Res Commun. 2006; 344:814–820. [PubMed: 16631607]
11. Yu H, Wu J, Potapova I, et al. MinK-related peptide 1: a beta subunit for the HCN ion channel subunit family enhances expression and speeds activation. Circ Res. 2001; 88:E84–E87. [PubMed: 11420311]
12. McCrossan ZA, Roepke TK, Lewis A, Panaghie G, Abbott GW. Regulation of the Kv2.1 potassium channel by MinK and MiRP1. J Membr Biol. 2009; 228:1–14. [PubMed: 19219384]
13. Zhang M, Jiang M, Tseng GN. MinK-related peptide 1 associates with Kv4.2 and modulates its gating function: potential role as beta subunit of cardiac transient outward channel? Circ Res. 2001; 88:1012–1019. [PubMed: 11375270]
14. Delpon E, Cordeiro JM, Nunez L, et al. Functional effects of KCNE3 mutation and its role in the development of Brugada syndrome. Circ Arrhythm Electro-physiol. 2008; 1:209–218.
15. Roepke TK, Kontogeorgis A, Ovanez C, et al. Targeted deletion of *KCNE2* impairs ventricular repolarization via disruption of $I_{K,s}$low1 and I_{to},f. FASEB J. 2008; 22:3648–3660. [PubMed: 18603586]
16. Calloe K, Cordeiro JM, Di Diego JM, et al. A transient outward potassium current activator recapitulates the electrocardiographic manifestations of Brugada syndrome. Cardiovasc Res. 2009; 81:686–694. [PubMed: 19073629]
17. Dixon JE, Shi W, Wang HS, et al. Role of the Kv4.3 K^+ channel in ventricular muscle. A molecular correlate for the transient outward current. Circ Res. 1996; 79:659–668. [PubMed: 8831489]

18. Kääb S, Dixon J, Duc J, et al. Molecular basis of transient outward potassium current downregulation in human heart failure: a decrease in Kv4.3 mRNA correlates with a reduction in current density. Circulation. 1998; 98:1383–1393. [PubMed: 9760292]
19. Benitah JP, Gomez AM, Bailly P, et al. Heterogeneity of the early outward current in ventricular cells isolated from normal and hypertrophied rat hearts. J Physiol. 1993; 469:111–138. [PubMed: 7505822]
20. Singleton CB, Valenzuela SM, Walker BD, et al. Blockade by N-3 polyunsaturated fatty acid of the Kv4.3 current stably expressed in Chinese hamster ovary cells. Br J Pharmacol. 1999; 127:941–948. [PubMed: 10433502]
21. Deschênes I, Tomaselli GF. Modulation of Kv4.3 current by accessory subunits. FEBS Lett. 2002; 528:183–188. [PubMed: 12297301]
22. Wang S, Bondarenko VE, Qu Y, Morales MJ, Rasmusson RL, Strauss HC. Activation properties of Kv4.3 channels: time, voltage and $[K^+]_o$ dependence. J Physiol. 2004; 557:705–717. [PubMed: 15004209]
23. An WF, Bowlby MR, Betty M, et al. Modulation of A-type potassium channels by a family of calcium sensors. Nature. 2000; 403:553–556. [PubMed: 10676964]
24. Decher N, Uyguner O, Scherer CR, et al. hKChIP2b is a functional modifier of hKv4.3 potassium channels: cloning and expression of a short hKChIP2b splice variant. Cardiovasc Res. 2001; 52:255–264. [PubMed: 11684073]
25. Radicke S, Cotella D, Graf EM, et al. Functional modulation of the transient outward current I_{to} by *KCNE* beta-subunits and regional distribution in human non-failing and failing hearts. Cardiovasc Res. 2006; 1:695–703. [PubMed: 16876774]
26. Deschênes I, DiSilvestre D, Juang GJ, Wu RC, An WF, Tomaselli GF. Regulation of Kv4.3 current by KChIP2b splice variants: a component of native cardiac I_{to}? Circulation. 2002; 106:423–429. [PubMed: 12135940]
27. Radicke R, Vaquero M, Caballero R, et al. Effects of MiRP1 and DPP6 β-subunits on the blockade induced by flecainide of Kv4.3/KChIP2 channels. Br J Pharmacol. 2008; 154:774–786. [PubMed: 18536731]
28. Wettwer E, Amos GJ, Posival H, Ravens U. Transient outward current in human ventricular myocytes of subepicardial and subendocardial origin. Circ Res. 1994; 75:473–482. [PubMed: 8062421]
29. Patel SP, Campbell DL. Transient outward potassium current, "I_{to}," phenotypes in the mammalian left ventricle: underlying molecular, cellular and biophysical mechanisms. J Physiol. 2005; 569:7–39. [PubMed: 15831535]
30. Antzelevitch C. Brugada syndrome. Pacing Clin Electrophysiol. 2006; 29:1130–1159. [PubMed: 17038146]
31. Bezzina C, Veldkamp MW, van den Berg MP, et al. A single Na^+ channel mutation causing both long-QT and Brugada syndromes. Circ Res. 1999; 85:1206–1213. [PubMed: 10590249]
32. Van den Berg MP, Wilde AA, Viersma TJW, et al. Possible bradycardic mode of death and successful pacemaker treatment in a large family with features of long QT syndrome type 3 and Brugada syndrome. J Cardiovasc Electrophysiol. 2001; 12:630–636. [PubMed: 11405394]

Abbreviations

CHO	Chinese hamster ovary
HERG	human ether-a-go-go related gene
WT	wild type

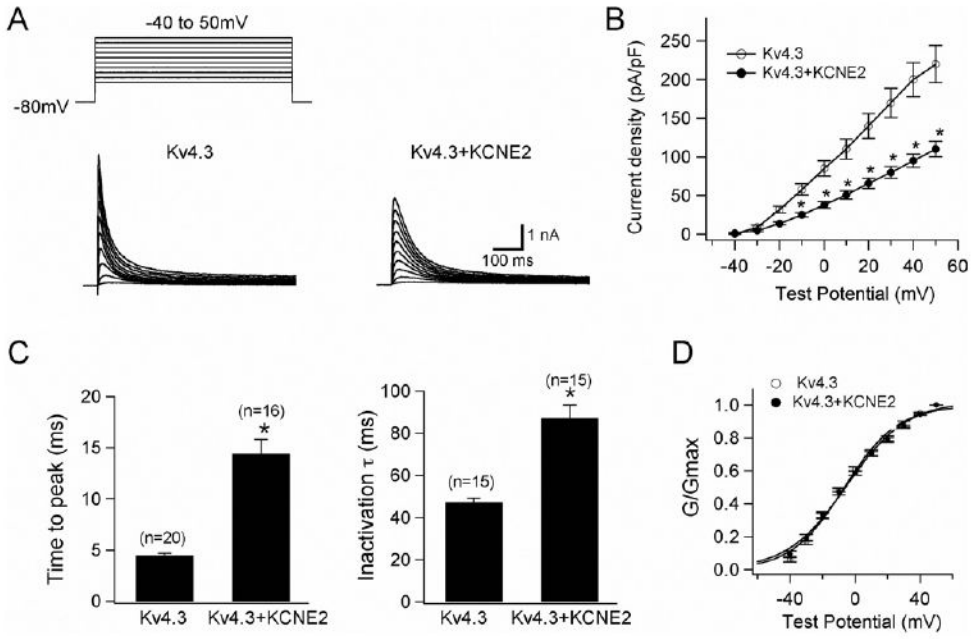

Figure 1.

KCNE2 co-expression with Kv4.3 produces smaller I_{to}-like currents with slower activation/inactivation kinetics. **A:** Representative current traces recorded from Chinese hamster ovary (CHO) cells expressing Kv4.3 **(left)** and Kv4.3 + *KCNE2* **(right).** As shown in the **inset** in panel A, depolarizing step pulses of 1-second duration were introduced from a holding potential of −80 mV to potentials ranging from −40 to +50 mV in 10-mV increments. **B:** Current–voltage relationship curve showing peak current densities in the absence and presence of co-transfected *KCNE2* (**P* <.05 vs Kv4.3). **C:** Bar graphs showing the kinetic properties of reconstituted channel currents: time to peak of activation course **(left)** and inactivation time constants **(right)** measured using test potential to +20 mV (**P* <.05 vs Kv4.3). Numbers in parentheses indicate numbers of experiments. **D:** Normalized conductance–voltage relationship for peak outward current of Kv4.3 and Kv4.3 + *KCNE2* channels.

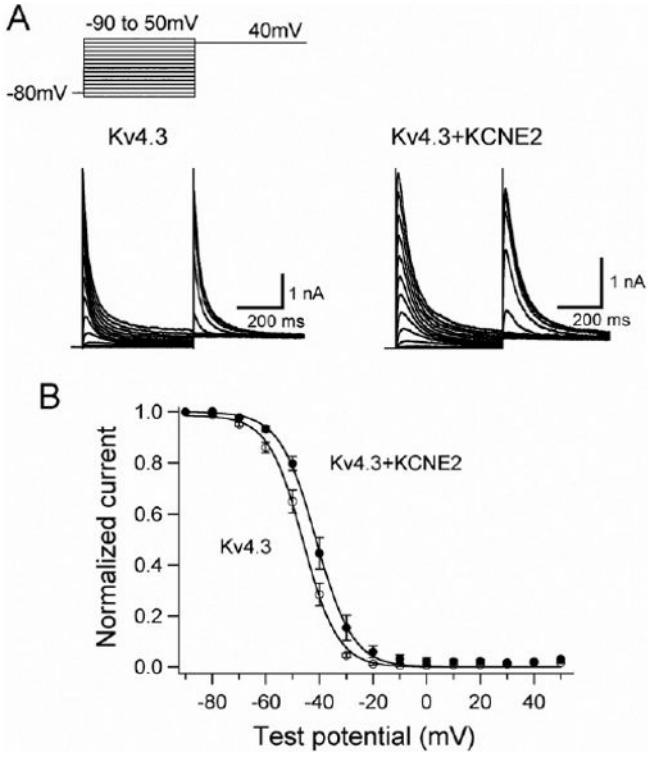

Figure 2.

KCNE2 co-expression with Kv4.3 causes a positive shift of voltage dependence of steady-state inactivation. **A:** Representative Kv4.3 and Kv4.3 + *KCNE2* current traces induced by 500-ms pulses (P1) from −90 to +50 mV applied from the holding potential −80 mV in 10-mV steps followed by a second pulse (P2) to +40 mV. **B:** Steady-state inactivation curves for Kv4.3 (*open circles*) and Kv4.3 + *KCNE2 (closed circles*) channels.

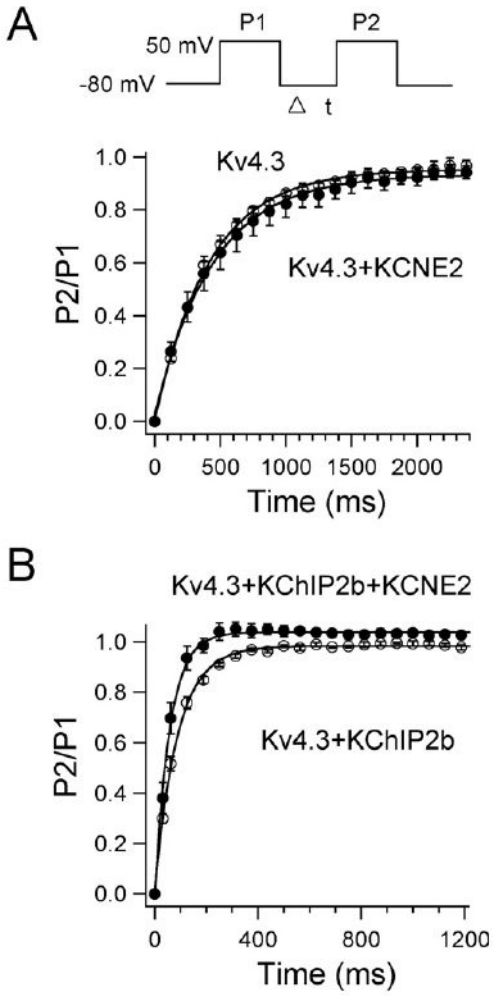

Figure 3.

Effects of *KCNE2* co-expression on recovery from inactivation of Kv4.3 **(A)** and Kv4.3 + KChIP2b **(B)** currents. Recovery from inactivation was assessed by a two-pulse protocol **(A, inset):** a 400-ms test pulse to +50 mV (P1) followed by a variable interval at −80 mV, then by a second test pulse to +50 mV (P2). Data were fit to a single exponential.

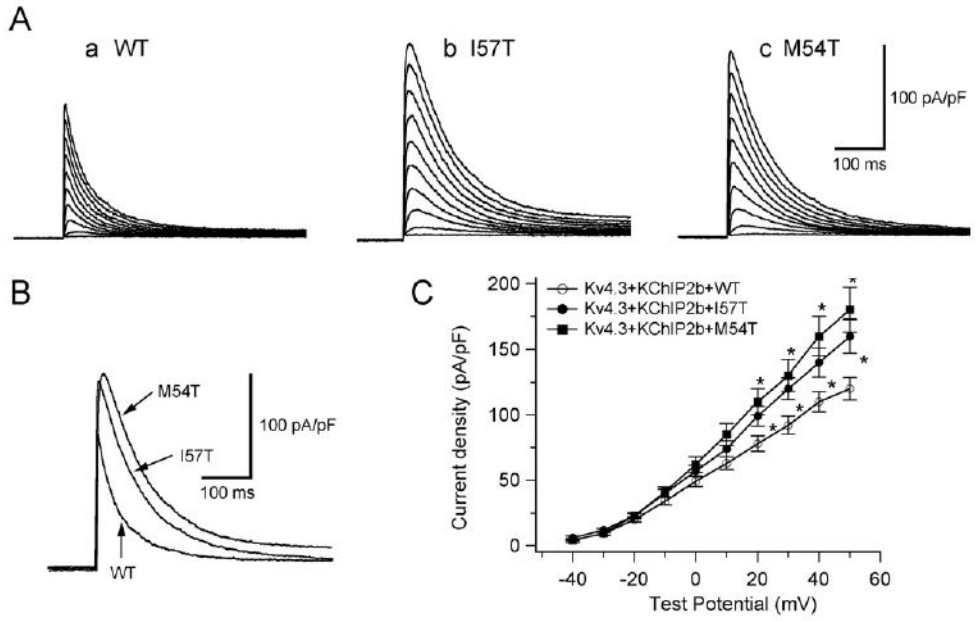

Figure 4.

Two *KCNE2* transmembrane variants, I57T and M54T, increase the reconstituted Kv4.3 + KChIP2b channel current and slow its inactivation. **A:** Three sets of current traces elicited by depolarizing pulses for 500 ms from a holding potential of −80 mV to potentials ranging between −40 and +50 mV in 10-mV increments (same protocol as in experiments of Figure 1A). **B:** Superimposition of three original current traces recorded upon depolarization showing variant-related increase in peak outward current density. **C:** Current–voltage relationship curve showing average peak outward current densities (**P* <.05 vs Kv4.3 + KChIP2b + WT). WT = wild type.

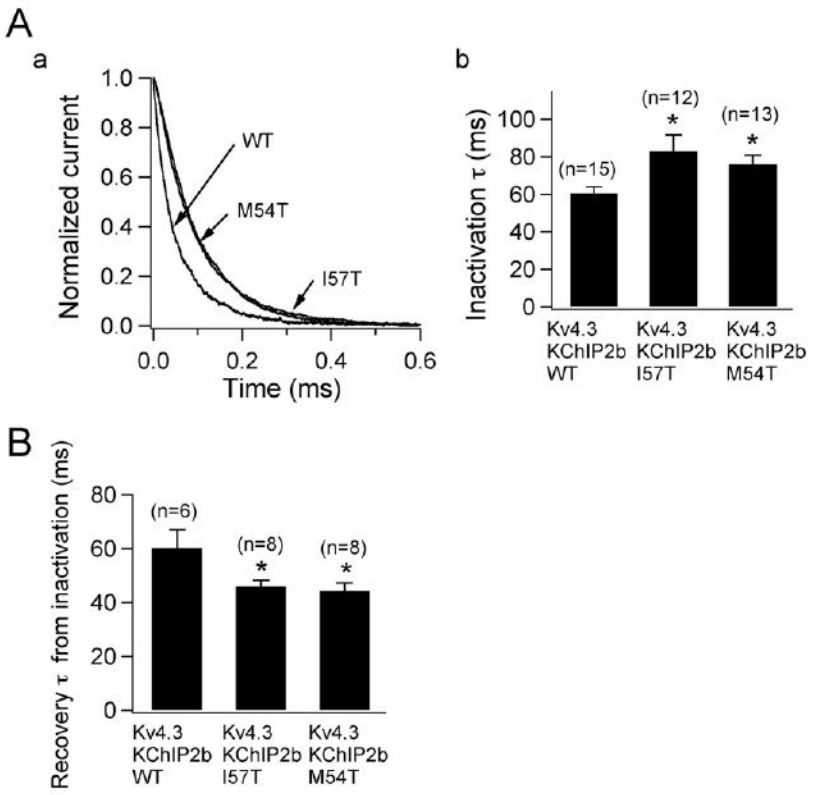

Figure 5.

Two *KCNE2* variants slow inactivation kinetics and accelerate recovery from inactivation. **A, a:** Three current traces obtained from Chinese hamster ovary (CHO) cells transfected with wild-type (WT), I57T, and M54T *KCNE2* variant co-expressed with Kv4.3 and KChIP2b. Traces, which are normalized and superimposed, show that the variants slow inactivation. **A, b:** Time constants of decay at +20 mV for WT and variant *KCNE2* (**P* <.05 vs Kv4.3 + KChIP2b + WT). Numbers in parentheses indicate numbers of observations. **B:** Time constants of recovery from inactivation recorded using a double-pulse protocol (**P* <. 05 vs Kv4.3 + KChIP2b + WT). Numbers in parentheses indicate numbers of observations.

Table 1

Effects of *KCNE2* on Kv4.3 and Kv4.3 + KChIP2b

Parameter	Kv4.3	Kv4.3 *KCNE2*	Kv4.3 KChIP2b	Kv4.3 KChIP2b *KCNE2*
Current density at +20 mV (pA/pF)	142.0 ± 16.0 (n = 12)	66.0 ± 6.6* (n = 12)	191.5 ± 33.8 (n = 15)	77.8 ± 5.9† (n = 20)
Steady-state activation ($V_{0.5}$ in mV)	−6.5 ± 2.1 (n = 9)	−5.5 ± 1.7 (n = 11)	−7.5 ± 1.7 (n = 8)	−7.4 ± 1.4 (n = 8)
Steady-state inactivation ($V_{0.5}$ in mV)	−46.0 ± 1.3 (n = 10)	−40.8 ± 1.7* (n = 8)	−49.8 ± 1.4 (n = 7)	−44.5 ± 1.9*† (n = 7)
τ of inactivation at +20 mV (τ_{inact} in ms)	47.3 ± 2.0 (n = 15)	87.2 ± 6.2* (n = 15)	47.5 ± 2.2 (n = 15)	66.6 ± 3.5† (n = 15)
Time to peak at +50 mV (TtP in ms)	4.5 ± 0.2 (n = 20)	14.4 ± 1.4* (n = 16)	4.1 ± 0.2 (n = 15)	6.1 ± 0.5† (n = 21)
τ of recovery from inactivation (ms)	419.6 ± 18.8 (n = 6)	485.6 ± 74.8 (n = 6)	89.2 ± 5.3 (n = 6)	60.2 ± 6.9† (n = 6)

*Significantly different from Kv4.3.

†Significantly different from Kv4.3 + KChIP2b.